2025 IEEE/ASME International Conference on Advanced Intelligent Mechatronics (AIM) | 979-8-3315-3342-7/25/$31.00 ©2025 IEEE | DOI: 10.1109/AIM64088.2025.11175814

Adaptive Transmission Power for Robust and Energy-Efficient Bluetooth Communication in Dynamic Environments

Ziyao Zhou[1], Hen-Wei Huang[1,2]

***Abstract*—Wireless communication is ubiquitous in our daily life, with Bluetooth Low Energy (BLE) being a key protocol in the mobile Internet of Things (IoT). However, BLE data throughput is highly sensitive to signal quality, and conventional approaches often maximize transmission power (TXP) to maintain high link quality, which will lead to energy inefficiency and will further reduce peripheral devices' battery lifetime. In this work, we implement a Proportional-Integral-Derivative (PID) control loop between a central and a peripheral device to dynamically reconfigure the peripheral device's TXP based on real-time feedback from the central device's Received Signal Strength Indicator (RSSI). Our findings indicate that data throughput significantly declines only when RSSI is near the central device's sensitivity threshold (-89 dBm for nRF52833). By maintaining a central device with an RSSI of -60 dBm in a varying distance ranging from 0 to 50 meters, our PID-controlled system reduces power consumption by 2.5 times compared to a non-PID peripheral device operating at a fixed TXP of 20 dBm without compromising data throughput. In addition, compared to a fixed TXP of -10 dBm, the PID system greatly mitigates the risk of disconnection and drop of data rate, with only a 20% increase of power consumption.**

***Index Terms*—PID, BLE, Wireless Communication, RSSI, Data Throughput, Power Consumption**

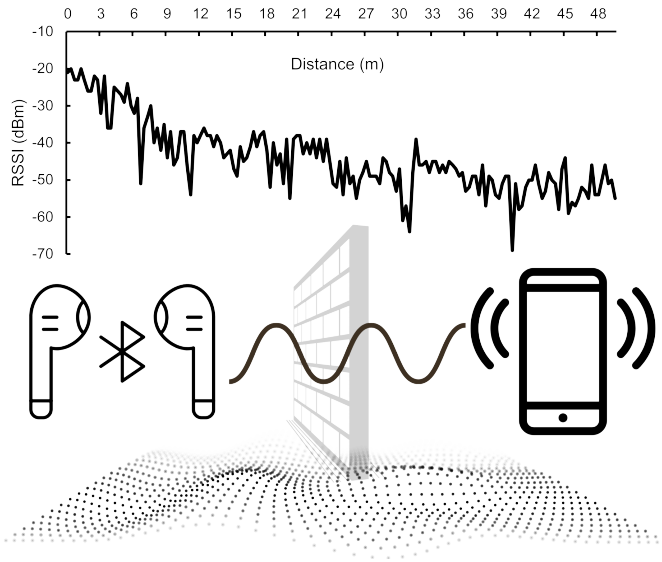

Fig. 1: RSSI varies with distance. The RSSI fluctuates due to shadowing, fading, and path loss when using BLE devices.

I. Introduction

Wireless communication technologies have become fundamental to modern life. Bluetooth stands out due to its wide device compatibility, low energy consumption, and high data throughput. It supports data rates up to 3 Mbps and typically consumes 100 mW [1]. Bluetooth Low Energy (BLE), a subset of Bluetooth explicitly designed for ultra-low power consumption, is approximately 10 mW with a maximum data rate of 2 Mbps, making it ideal for mobile Internet of Things (IoT) devices [2]–[6].

BLE applications have diverse throughput requirements, necessitating careful selection of communication parameters to optimize both performance and energy efficiency. For example, motion detection requires approximately 10 kbps for 100 Hz sampling, whereas LE Audio, utilizing the LC3 codec, demands up to 320 kbps with a 10 ms frame duration [7]. To ensure high quality of service, the system's data throughput must exceed the target application's requirements, providing a reliable and consistent communication performance.

Several algorithms have been developed to optimize power consumption while maintaining communication throughput in the 2.4 GHz range. One of the most notable is AdaptaBLE, a BLE-specific solution introduced in [8], which regulates transmission power (TXP) based on the Packet Reception Ratio (PRR). While effective in low-frequency data transmission scenarios, such as motion detection, AdaptaBLE lacks the result in high-bandwidth applications. Furthermore, its reliance on a non-robust conditional judgment control algorithm limits its adaptability to dynamic environments, and the PRR metric, which is derived over extended periods, constrains real-time responsiveness.

Another relevant approach is Adaptive Transmission Power Control (ATPC), proposed in [9], which utilizes a rapidly updated Received Signal Strength Indicator (RSSI) and Link Quality Indicator (LQI) feedback to optimize energy efficiency while maintaining link quality. ATPC employs a closed-loop control mechanism for dynamic transmission power adjustment. However, its reliance on LQI, defined in IEEE 802.15.4

[1]School of Electrical and Electronic Engineering, Nanyang Technological University, Singapore
[2]LKC School of Medicine, Nanyang Technological University, Singapore
ZHOU0557@e.ntu.edu.sg
henwei.huang@ntu.edu.sg

[10], restricts its applicability to BLE-based communication systems, where LQI is unavailable.

RSSI used in ATPC is often considered an unreliable metric for directly determining optimal transmission rates due to its inherent inaccuracies in reflecting channel quality [11]. However, it remains strongly correlated with achievable throughput [9], [12], [13]. As illustrated in Fig. 1, RSSI variations in dynamic environments are influenced by three components: shadowing, fading, and path loss [14]. These factors introduce fluctuations, making RSSI inherently unstable.

In this work, we propose a closed-loop TXP control strategy using a PID controller implemented on a central device. The controller dynamically adjusts the TXP of a peripheral device based on fast-updated RSSI feedback from the central device. This approach aims to minimize the peripheral device's power consumption while maintaining optimal data throughput in high-bandwidth applications. This study will explore the relationship between RSSI and data throughput, analyze system power consumption across different TXP levels, and evaluate the effectiveness of the PID controller in optimizing energy efficiency.

II. Methodology

In our methodology, we first analyzed the correlation between RSSI and throughput and examined power consumption at different TXP levels. We then implemented a PID-based closed-loop control system that dynamically adjusts TXP based on real-time RSSI feedback.

A. Relationship between Throughput and RSSI

We conducted experiments using four Nordic nRF52833 DK development boards, configured into two central-peripheral device pairs, to analyze the relationship between RSSI and throughput. The peripheral and central devices in each pair were placed adjacent to each other to ensure consistent testing conditions.

One device pair operated Nordic's official Bluetooth UART sample, where the central device measured the RSSI value of its connection with the peripheral device every 100 ms. The second pair ran the Bluetooth Throughput sample code, using the following parameters:

- ATT MTU size: 498 bytes
- Data length: 251 bytes
- Connection interval: 320 units (400 ms)
- Physical layer (PHY) data rate: 2 Mbps

The experiments were conducted on an open, spacious rooftop to minimize environmental interference. To ensure controlled and repeatable conditions, the UART-central and Throughput-central devices were mounted on a mobile platform, while the two peripheral devices remained fixed on a table. During the tests, the distance between the central and peripheral devices was continuously varied to induce changes in the received RSSI values.

Both device pairs were configured with identical parameters, including a TXP of 0 dBm, ensuring that the RSSI of the Throughput pair could be represented by that from the UART pair.

To systematically evaluate throughput performance under varying signal conditions, we targeted seven RSSI levels ranging from -20 dBm to -80 dBm in 10 dB increments. A target RSSI value was considered reached when the measured RSSI fluctuated within ±5 dB of the desired level. Once stabilized, a Bluetooth Throughput test was conducted at that specific RSSI. Each RSSI evaluation test was repeated three times to ensure the consistency and reliability of the measurements.

B. Power Consumption with Varying TXP

The power consumption of a BLE device is directly influenced by its TXP and data rate [8]. The nRF52833 supports a configurable TXP range from -40 dBm to 8 dBm [15]. To extend this range, we added nRF21540 RF front-end module (FEM) to boost the TXP with a new range from -30 dBm to 20 dBm [16].

To evaluate power consumption under high-bandwidth conditions, we conducted experiments where the system continuously transmitted 244-byte strings using the Nordic UART Service (NUS). The communication parameters remained consistent with those used in the Bluetooth Throughput sample.

Initially, the peripheral and central devices were placed nearby in an indoor environment to conduct the test. A Nordic Power Profiler Kit II (PPK) was connected to the peripheral device as an external power supply, providing a stable 1.8 volt while precisely measuring power consumption at a sampling rate of 100,000 samples per second.

We then increased the separation between the devices to 8 meters and repeated the high-bandwidth test. This environment included shelves and electrical appliances, introducing potential signal scattering and attenuation, simulating a realistic static testing scenario. With increased distance, packet loss rates typically rise, potentially leading to connection failures and intermittent radio inactivity, which could influence the system's overall power consumption.

C. PID Controller Deployment

Our PID system setup consists of two loops, shown in Fig. 2. The first loop, denoted in a dashed line, handles data generation, transmission, and utilization, aiming for a target BLE application.

The second loop, denoted in a solid line, is a closed-loop PID controller. On the central side, we continuously measure the RSSI and store it in a buffer for filtering before feeding the processed value into the PID controller. The PID controller calculates the appropriate TXP for the next transmission and updates the peripheral device accordingly. All processing is performed on the central device to minimize computational overhead and power consumption on the peripheral device.

We utilize the nRF Connect SDK's built-in function for real-time RSSI measurements. The nRF52833 updates RSSI values within 15 microseconds upon signal level changes [15]. The TXP range is set from -10 dBm to 20 dBm, as values between

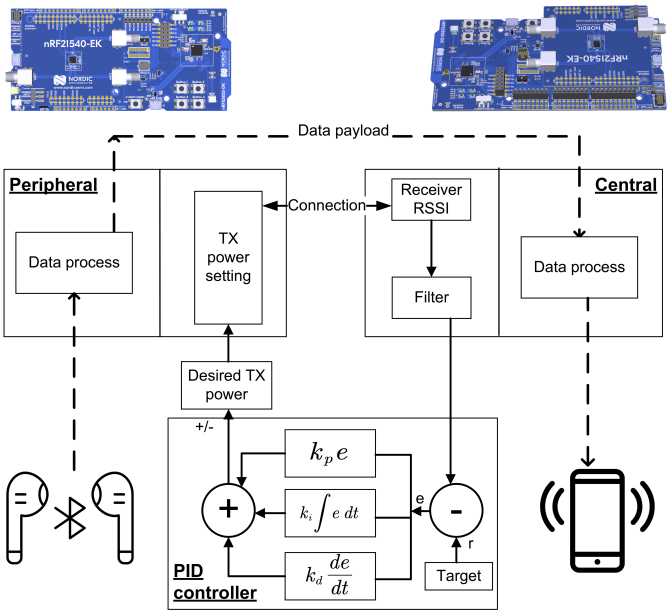

Fig. 2: The PID controller block diagram. The dashed line connections represent the data transmission part, while the solid line connections represent the PID closed-loop control part.

-10 dBm and -30 dBm are not configurable due to the FEM characteristics.

To ensure stability while capturing dynamic signal variations, we designed a moving average filter with a size of two. This filter computes the average of the current and previous RSSI values, providing a balance between responsiveness and stability.

Regarding the PID controller, we utilized the proportional (P) and integral (I) parameters for control. The peripheral and central devices were placed in fixed positions under consistent environmental conditions for the parameter choosing. By tuning the parameters, we identified the optimal values that maintained the target number and minimized the standard deviation of the RSSI, specifically $k_p = 0.2$, $k_i = 0.01$, and $k_d = 0$ with target -60 dBm. Additionally, we set the PID output limit to 5, ensuring that the system quickly converges to the target value without excessive overshoot.

We then placed the central and peripheral devices 8 meters apart in the same indoor environment described in the previous section. Under this static condition, we conducted experiments to analyze the effects of the filter and the PID computing frequencies (disabled, 1 Hz, 10 Hz, and 100 Hz). Specifically, for the disabled test, the TXP was set to -10 dBm and 20 dBm to see the difference.

To emulate rapid dynamic environmental changes affecting signal quality, we introduced a controlled RSSI disturbance by performing a plug-in and plug-out of the FEM on the central device. The nRF21540 FEM provides a 13 dB gain at the central device's receiving end [16], leading to a sudden and significant change in RSSI. During this process, we continuously monitored the central device's RSSI to evaluate the system's response to the disturbance. The primary objective was to measure the time required for the PID controller to stabilize the system and restore the RSSI to the target value following the 13 dB fluctuation induced by the FEM connection change.

We finally placed the peripheral device on a controlled platform and moved it away from the central device at a constant speed of 0.3 m/s in an open corridor. This setup simulated a dynamic communication scenario, where signal strength progressively weakens over time. During the experiment, we also used the PPK to record the peripheral device's power consumption continuously. Simultaneously, the central device logged real-time RSSI values, allowing us to analyze how TXP adjustments affected both power and signal stability in response to increasing distance. This experiment aimed to evaluate the PID controller's effectiveness in dynamically optimizing TXP while maintaining a stable communication link under changing environmental conditions.

III. RESULTS AND DISCUSSION

A. Relationship between Throughput and RSSI

The relationship between data throughput and RSSI is illustrated in Fig. 3. When RSSI is above -70 dBm, throughput remains relatively stable, exceeding 1000 kbps, which is sufficient for high-bandwidth data transfer [17]. However, once RSSI drops to -80 dBm, throughput declines sharply. Our outdoor experimental results align with trends observed in [18] for 2M PHY indoor environments and [19] for 1M PHY indoor environments, demonstrating the consistent impact of RSSI on throughput across different conditions.

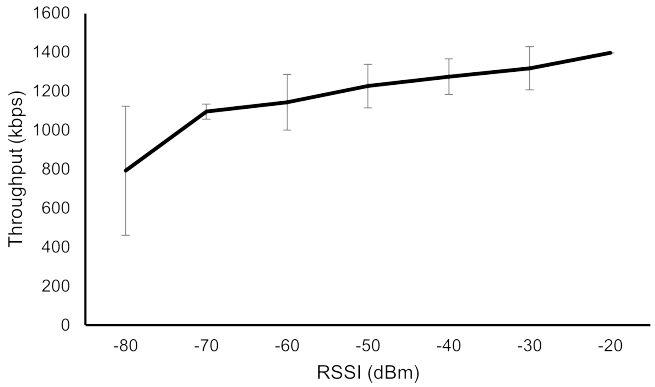

Fig. 3: Relationship between throughput and RSSI. Above -70 dBm, the curve remains stable with a slow increase. At -80 dBm, it drops sharply.

Our results indicate that for high-bandwidth communication in a given environment, a wide range of TXP settings can sustain the target throughput as long as the central device's RSSI remains above the receiver sensitivity threshold. If RSSI approaches this threshold, packet loss increases significantly, leading to a sharp decline in communication performance. Maintaining a stable RSSI above the sensitivity level is therefore, crucial for ensuring reliable data transmission.

B. Power Consumption with Varying TXP

Fig. 4(a) illustrates the overall maximum current measured at 0 meters and 8 meters under varying TXP settings. Each

data transmission induces a peak current, which is recorded as the maximum current for that transmission. Increasing TXP from -10 dBm to 20 dBm results in a threefold increase in maximum current. However, no significant difference in the maximum current draw was observed between the two distances, indicating that environmental changes do not affect the peak current consumption.

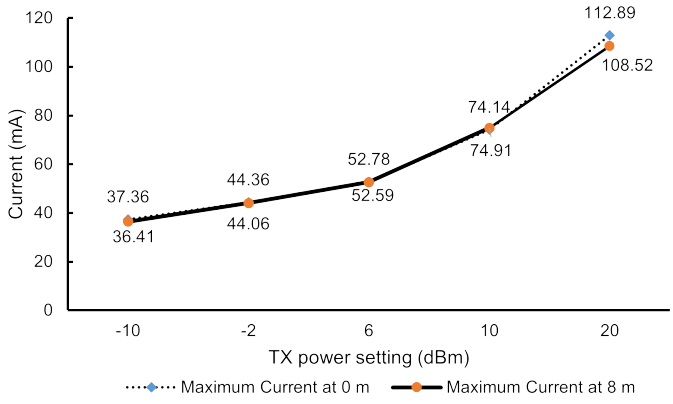

(a)

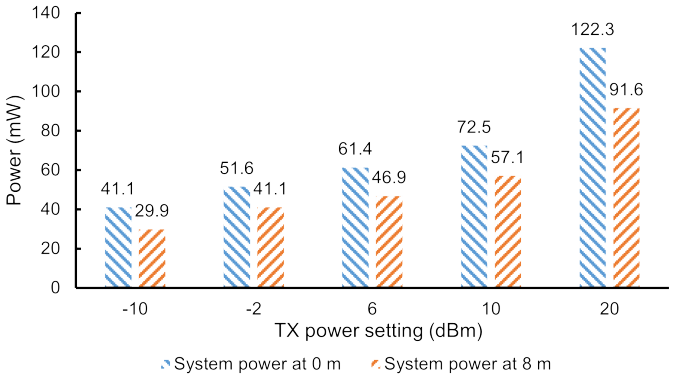

(b)

Fig. 4: (a). Overall maximum currents remain the same at 0 m and 8 m. (b). System power consumptions with different TXPs at 0 m and 8 m. Each TXP has a different system power level.

Fig. 4(b) illustrates that average transmission power consumption increases proportionally with TXP. The trend closely follows that of the maximum current draw, where increasing TXP from -10 dBm to 20 dBm results in a threefold rise in power consumption at both distances. However, for a fixed TXP, average power consumption differs between the two distances, with longer distances leading to lower power consumption.

This reduction can be attributed to packet loss. In a BLE connection, each connection interval starts with a packet transmission. If the packet has been successfully transmitted, the transmitter receives the correct CRC, and the next packet is sent immediately within the same interval. However, if CRC errors occur (e.g., due to noise), the peripheral must retransmit the packet in the next connection interval, leading to idle time between connection events. This behavior reduces the number of packets sent per interval, keeping the radio inactive for extended periods and thereby lowering power consumption.

In the RSSI vs. throughput experiment, we observed that throughput remained relatively stable across RSSI values from -70 dBm to -20 dBm. This suggests that reduced TXP with a proper central device's RSSI can sustain an acceptable throughput level, enabling significant power savings. For instance, if TXP was reduced from 20 dBm to -10 dBm, we could achieve a 66.9% reduction in power consumption, significantly improving the peripheral device's energy efficiency.

At -80 dBm, however, throughput degraded significantly, and the system became prone to disconnection, as this RSSI value is close to the 2M PHY RX sensitivity (-89 dBm). Given that the central device's FEM provides a 13 dB gain, the RSSI must be maintained above -67 dBm to prevent unexpected disconnections in case of FEM detachment. Based on these findings, we selected -60 dBm as the target RSSI for the PID controller in the subsequent experiments.

C. PID Controller Depolyment

The first experiment to validate the PID controller was conducted in a static indoor setting, with the peripheral and central devices positioned 8 meters apart in a laboratory environment. This setup simulated a typical indoor communication scenario, allowing us to assess signal behavior in the presence of various obstacles and evaluate the ability of the PID controller to dynamically adjust TXP to maintain stable RSSI.

From the experimental results shown in Table I, PID is turned on with Kp = 0.2 and Ki = 0.01. Neither the presence of a filter nor the PID update frequency significantly impacts the average RSSI. Across all six test conditions, the system consistently converges to approximately -60 dBm.

TABLE I: Comparison of central average RSSI and its standard deviation with and without a filter at different PID calculation frequencies.

	With Filter			**Without Filter**		
Frequency	100Hz	10Hz	1Hz	100Hz	10Hz	1Hz
Avg	-59.98	-60.11	-58.80	-59.84	-60.11	-59.57
STD	4.38	4.82	5.35	4.50	5.03	5.72

The filter effectively stabilized RSSI fluctuations, reducing the overall RSSI standard deviation by 0.1 to 0.3 across different update frequencies. Higher update frequencies improved RSSI stability by enabling more precise link quality monitoring and a faster system response. The best stability was achieved at 100 Hz, where the standard deviation was reduced to 4.38 with the filter applied.

In the next experiment, shown in Fig. 5, we applied the optimal 100 Hz filtered setup to compare performance with and without PID control. The dot represents the mean RSSI, while the dashed line indicates the median RSSI. With PID enabled, both the mean and median values aligned at the target -60 dBm, demonstrating the controller's effectiveness in tracking target value.

For comparison, we conducted two additional tests with PID disabled, using fixed TXP levels of 20 dBm and -10 dBm.

The results showed that RSSI fluctuations were significantly larger at 20 dBm TXP compared to the PID-controlled case. Additionally, the mean and median RSSI values differed in both fixed TXP conditions, highlighting inconsistent signal stability. These findings confirm that PID control not only stabilizes RSSI fluctuations but also ensures it remains close to the target RSSI.

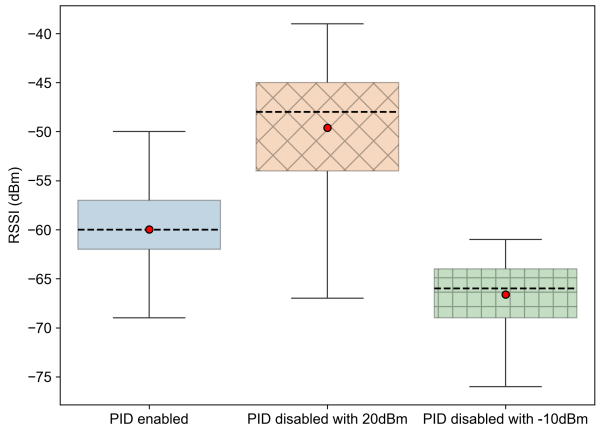

Fig. 5: Central device's RSSI variation in static state. The dot represents the mean, while the broken line represents the median. PID controller keeps the mean and median both at -60 dBm.

In the next phase, we introduced ±13 dB disturbances to the system by plugging in and unplugging the FEM, allowing us to evaluate the PID controller's dynamic response. As shown in Fig. 6(a), plugging in the FEM caused an instantaneous 13 dB increase in the central device's RSSI. The PID controller immediately responded, rapidly adjusting TXP by reducing 16 dB (from 12 dBm to -4 dBm), stabilizing the RSSI around -60 dBm within 110 ms.

Conversely, unplugging the FEM caused the RSSI to drop by 13 dB, prompting the peripheral device to compensate by increasing its TXP by 12 dB (from -6 dBm to 6 dBm) to restore stability. As with the plug-in scenario, the PID controller responded immediately and adapted to the RSSI drop within 100 ms. These results confirm the PID controller's effectiveness in dynamically adjusting TXP to sudden signal variations, ensuring stable communication under rapidly changing conditions.

Finally, in the dynamic experiment, we validated the benefits of PID control in two key aspects: stabilizing the RSSI to ensure a consistent throughput and reducing power consumption.

TABLE II: Average system power variation with or without PID activation during motion.

Configuration	Average Power Consumption (mW)
PID enabled	38.05
PID disabled (-10 dBm)	31.63
PID disabled (20 dBm)	90.88

As shown in Fig. 7(a), when PID was enabled (the blue points), after a 20 m distance, the RSSI finally reached and

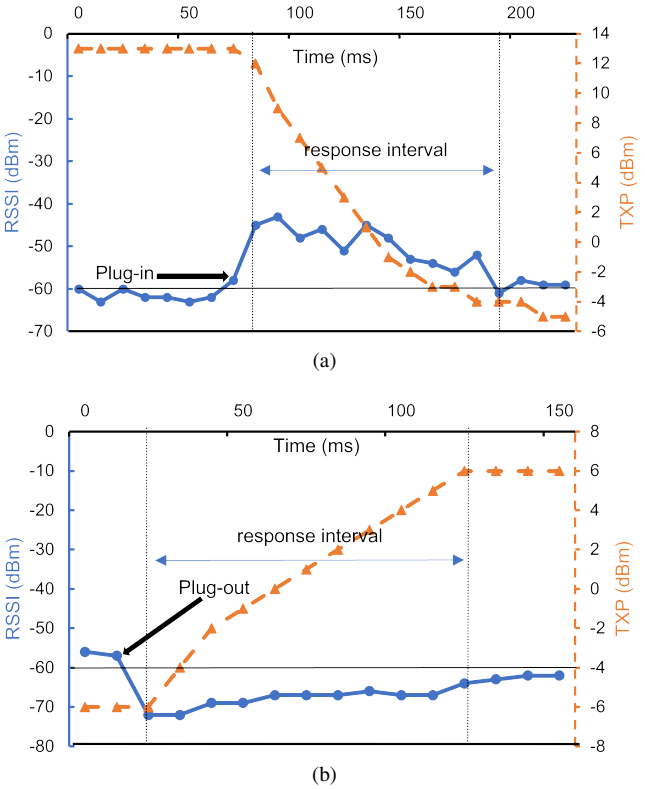

Fig. 6: Dynamic response of PID control when FEM plugged in (a) and plugged out (b). The dot represents the central device's RSSI, while the triangle symbol represents the TXP. The interval between each symbol is 10 ms (at 100 Hz), and the symbols are connected by lines to indicate the changing trend. PID controller fast adapts to - 60 dBm around 100 ms.

fluctuated around -60 dBm without showing a downward trend. However, the RSSI exhibited a continuous decline and significant variations for fixed TXP levels of 20 dBm and -10 dBm. For TXP = -10 dBm, the received RSSI approached -80 dBm, leading to a substantial decrease in throughput. In contrast, with PID control, only a few outliers dropped close to -70 dBm, while the majority of measurements remained around -60 dBm. At this range, the throughput would be stable.

Fig. 7(b) shows the power consumption at every 10-meter point. It can be observed that when PID is disabled, using a fixed -10 dBm or 20 dBm, both exhibit a decreasing trend, which is due to the mild packet loss discussed earlier. When PID is enabled, the power consumption at short distances is similar to that of -10 dBm, as the signal is strong enough, causing PID to use the minimum TXP (-10 dBm). After 20 m, power consumption increases, indicating that PID starts to increase TXP to stabilize to the target RSSI.

For TXP = 20 dBm, the overall average system power consumption was more than 2 times that of the PID-controlled case, reaching 90.9 mW, as shown in Table II. In addition, compared to a constant TXP of -10 dBm, the PID system only increases 20% power consumption. This result significantly highlights the ability of PID to reduce the power and maintain data throughput.

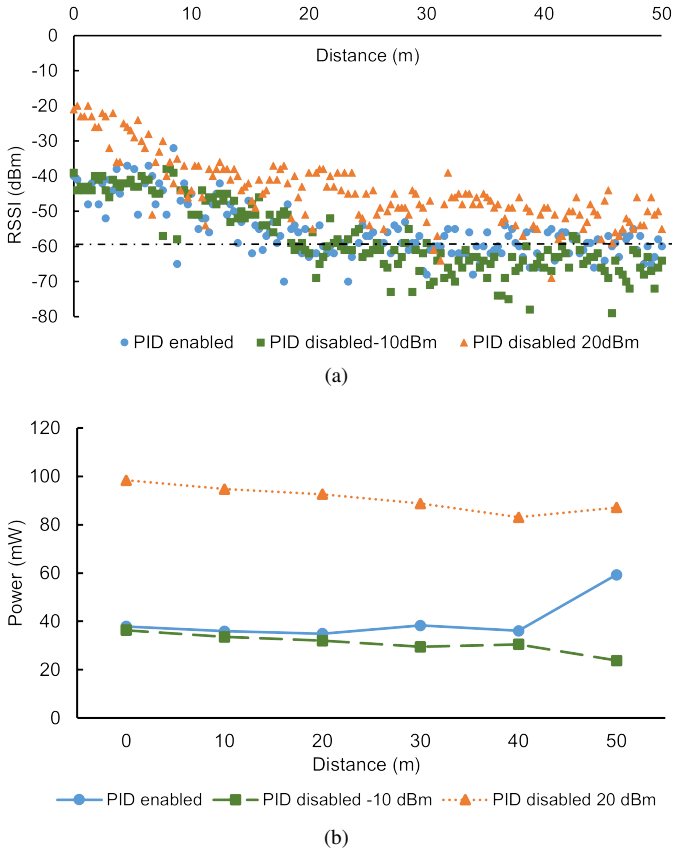

Fig. 7: (a).Variation of RSSI with distance under three different settings. (b). Instantaneous power changes with distance under three different settings. PID controller increased power at a far distance to maintain RSSI stability.

Conclusion and Future work

This study examined the relationship between RSSI and data throughput, demonstrating that as long as RSSI remains above a certain threshold, its direct effect on throughput is minimal. Traditional ways of using BLE often maximize TXP to maintain high link quality in dynamic environments. However, in high-bandwidth applications, increasing TXP leads to a trade-off between link quality and energy consumption, where higher TXP significantly increases power usage, posing challenges for low-power applications.

To address this, we developed a PID-based closed-loop control system that dynamically adjusts TXP to maintain the central device's RSSI within an optimal range while minimizing energy consumption. This approach effectively reduces power usage without compromising throughput, making it well-suited for energy-constrained BLE applications.

This method is particularly beneficial in scenarios requiring both robust BLE data transmission and power efficiency, such as capsule endoscopy, where sustaining high data throughput for video streaming must be balanced with battery longevity.

Future work could extend PID control to directly regulate throughput, providing a more intuitive and precise optimization strategy compared to the current method of modulating TXP to stabilize RSSI. By dynamically tracking throughput instead of RSSI, the system could achieve even greater efficiency and adaptability in BLE communication.

IV. Acknowledgement

This work was supported by the Nanyang Professorship and MOE Tier 1 grant RG71/24.

References

[1] H. Taleb, A. Nasser, A. Guillaume, N. Charara, and E. Cruz, "Wireless technologies, medical applications and future challenges in wban: a survey," *Wireless Networks*, vol. 27, 11 2021.

[2] L. Yuan, C. Xiong, S. Chen, and W. Gong, "Embracing self-powered wireless wearables for smart healthcare," in *2021 IEEE International Conference on Pervasive Computing and Communications (PerCom)*, pp. 1–7, 2021.

[3] F. Battaglia, G. Gugliandolo, G. Campobello, and N. Donato, "Eeg-over-ble: A low-latency, reliable, and low-power architecture for multichannel eeg monitoring systems," *IEEE Transactions on Instrumentation and Measurement*, vol. 72, pp. 1–10, 2023.

[4] S. Gautam and S. Kumar, "Low-power ble relay node operation in mesh-like architectures for precision agriculture," *IEEE Sensors Journal*, vol. 24, pp. 33347–33360, 2024.

[5] C. Liu, Y. Zhang, and H. Zhou, "A comprehensive study of bluetooth low energy," *Journal of Physics: Conference Series*, vol. 2093, p. 012021, 11 2021.

[6] M. Collotta, G. Pau, T. Talty, and O. K. Tonguz, "Bluetooth 5: A concrete step forward toward the iot," *IEEE Communications Magazine*, vol. 56, no. 7, pp. 125–131, 2018.

[7] Bluetooth SIG, Generic Audio Working Group, "Performance Characterization of the Low Complexity Communication Codec." White Paper, June 2023.

[8] E. Park, M.-S. Lee, and S. Bahk, "Adaptable: Data rate and transmission power adaptation for bluetooth low energy," in *2019 IEEE Global Communications Conference (GLOBECOM)*, pp. 1–6, 2019.

[9] S. Lin, F. Miao, J. Zhang, G. Zhou, L. Gu, T. He, J. A. Stankovic, S. Son, and G. J. Pappas, "Atpc: Adaptive transmission power control for wireless sensor networks," *ACM Trans. Sen. Netw.*, vol. 12, Mar. 2016.

[10] "Ieee standard for low-rate wireless networks," *IEEE Std 802.15.4-2024 (Revision of IEEE Std 802.15.4-2020)*, pp. 1–967, 2024.

[11] D. Halperin, W. Hu, A. Sheth, and D. Wetherall, "Predictable 802.11 packet delivery from wireless channel measurements," *SIGCOMM Comput. Commun. Rev.*, vol. 40, p. 159–170, Aug. 2010.

[12] L. Deek, E. Garcia-Villegas, E. Belding, S.-J. Lee, and K. Almeroth, "A practical framework for 802.11 mimo rate adaptation," *Computer Networks*, vol. 83, pp. 332–348, 2015.

[13] R. Maliwatu, A. Lysko, and D. Johnson, "Exploring rssi dependency on height in uhf for throughput optimization," in *2016 International Conference on Advances in Computing and Communication Engineering (ICACCE)*, pp. 7–12, 2016.

[14] Z. Ren, Y. Huang, Q. Chen, and H. Li, "Modeling and simulation of fading, pathloss, and shadowing in wireless networks," in *2009 IEEE International Conference on Communications Technology and Applications*, pp. 335–343, 2009.

[15] Nordic Semiconductor, *nRF52833 Product Specification v1.7*, June 2024.

[16] Nordic Semiconductor, *nRF21540 Product Specification v1.2*, January 2022.

[17] M. R. Soares, J. Oliveira, D. Correia, and R. Moutinho, "Characterizing in-body ble communication for high-bandwidth applications," in *2024 IEEE MTT-S International Microwave Biomedical Conference (IMBioC)*, pp. 75–77, 2024.

[18] B. Badihi, M. U. Sheikh, K. Ruttik, and R. Jäntti, "On performance evaluation of ble 5 in indoor environment: An experimental study," in *2020 IEEE 31st Annual International Symposium on Personal, Indoor and Mobile Radio Communications*, pp. 1–5, 2020.

[19] H. Karvonen, C. Pomalaza-Ráez, K. Mikhaylov, M. Hämäläinen, and J. Iinatti, "Experimental performance evaluation of ble 4 versus ble 5 in indoors and outdoors scenarios," in *Advances in Body Area Networks I* (G. Fortino and Z. Wang, eds.), (Cham), pp. 235–251, Springer International Publishing, 2019.